

# Maximizing Efficiency in Active Loudspeaker Systems

Wolfgang Klippel, KLIPPEL GmbH, Dresden, Germany

Increasing the efficiency of the electro-acoustical conversion is the key to modern audio devices generating the required sound output with minimum size, weight, cost and energy. There is unused potential for increasing the efficiency of the electro-dynamical transducer by using a nonlinear motor topology, a soft suspension and cultivating the modal resonances in the mechanical and acoustical system. However, transducers optimized for maximum efficiency are more prone to nonlinear and unstable behavior. Nonlinear adaptive control can compensate for the undesired signal distortion, protect the transducer against overload, stabilize the voice coil position and cope with time varying properties of the suspension. The paper discusses the design of modern active systems that combine the new opportunities provided by software algorithms with the optimization of the hardware components in the transducer and power amplifier.

## 1 Introduction

The user of loudspeakers, headphone and other audio devices expects that the audio signal can be reproduced at sufficient amplitude and quality but prefers products which are smaller, lighter, less cost intensive and provide a longer stand-alone operation in personal applications.

Creating such an audio product requires a combination of hardware and software components as illustrated in Figure 1.

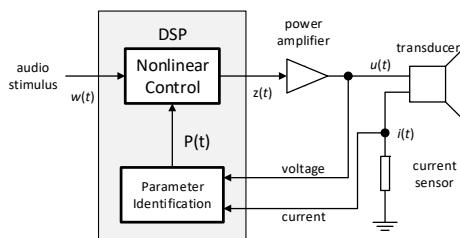


Figure 1: Active loudspeaker system with adaptive, nonlinear control of the transducer based on voltage and current monitoring

The next section gives an overview on the software algorithms that have been developed for loudspeakers. However, any electric control can only manipulate the audio input signal to exploit the existing hardware components (amplifier, transducer, enclosure). Additional benefits can be generated for the end user by using hardware components that are specially constructed for the opportunities provided by digital signal processing. This paper searches for new degrees of freedom in the hardware design to use all resources such as material, energy and manufacturing effort more efficiently (*Green Speaker Design*). The electro-acoustical efficiency is the important criterion for evaluating the final product and identifying weak points in the transducer design. For example, a typical micro-speaker converts the most of the electric energy into heat but only 0.01 % into sound power. Increasing efficiency is the key to generate more output by smaller loudspeaker systems and

reducing power consumption in portable applications with limited battery capacity.

For this discussion, the paper provides new definitions of the efficiency to consider the influence of the spectral properties of the complex audio signals (e.g. music). The paper explains the difference between efficiency and voltage sensitivity, which is a second important characteristic of the transducer required to match the transducer with the power amplifier.

After predicting the efficiency of an electro-dynamical transducer based on lumped parameter modeling in the small and large signal domain, the influence of the geometry and material properties will be discussed in greater detail. Finally, the new concept will be applied to a case study where the effect of a simple modification of an existing transducer will be investigated.

## 2 Loudspeaker Control

This section summarizes the new opportunities provided by digital signal processing for loudspeakers:

Linear filtering of the electric input signal has been used for a long time to equalize or align the overall amplitude and phase response at a receiving point and listening zone to a desired target curve [1]. The progress in amplification brought more power to the electric terminals than the transducer can handle. To avoid a mechanical and thermal overload, active protection systems have been developed that detect a critical state and attenuate the input signal before damage occurs. In order to combine reliable protection with maximum output, an accurate modeling of voice coil displacement and temperature at high amplitude is required [2]. Only a nonlinear model can explain the dynamic generation of a DC-displacement in the transducers which moves the coil away from the optimal position for maximum AC displacement [3]. Since the nonlinear behavior is predictable [4], it is obvious to use this knowledge in nonlinear controllers that generate a pre-distorted audio signal containing compensation distortion that cancels for the nonlinear distortion generated in the following loudspeaker. This leads to

a linear transfer behavior between control input and sound pressure output. The mirror filter [5] has a feed-forward structure and can be operated with fixed parameters, but any deviation between the control and transducer parameters will deteriorate the distortion cancelation. Therefore, loudspeakers require a self-learning control system that dispenses with a sophisticated tuning process and can react adaptively on production variances, aging of the suspension, changing climate conditions and other external influences [6]. Monitoring the input current and terminal voltage, as shown in Figure 1, provides reliable information [7] to identify the linear and nonlinear transducer parameters, the maximum excursion and the absolute rest position of the coil. If the power amplifier is DC coupled, the control system stabilizes the transducer [8] and keeps the coil at the optimal position, giving maximum AC displacement and sound output. The continuously updated transducer parameters are valuable information for transducer diagnostics to detect a deterioration process and anticipate a damage in order to initiate proper actions in time.

Nowadays, the cost generated by hosting software algorithms in silicon can compete with the benefits and cost savings generated on the transducer side, even in low-cost consumer applications.

### 3 Efficiency

The electro-acoustical efficiency of a loudspeaker, headphone or any other transducer is defined as ratio

$$\eta = \frac{P_a}{P_e} 100\% \quad (1)$$

between electric input power  $P_e$  and the acoustic output power  $P_a$  for any stimulus such as a test signal or common audio signals.

The real input power  $P_e$  can be calculated in the time domain as the product of input current  $i(t)$  and voltage  $u(t)$  averaged over a measurement interval or in the frequency domain as the integral of the cross-power density function  $S_{ui}(f)$ :

$$\begin{aligned} P_e &= \overline{u(t)i(t)} = \int_{-\infty}^{+\infty} S_{ui}(f) df \\ &= \int_{-\infty}^{+\infty} S_{uu}(f) \Re(\underline{Z}_E(f)^{-1}) df \end{aligned} \quad (2)$$

which is equivalent to the auto power spectrum of the stimulus  $S_{uu}(f)$  divided by the real part of the electric input impedance  $\underline{Z}_E(f)$ . The acoustic output power  $P_a$  can be determined by integrating the far field sound pressure over a closed surface  $S$  around the transducer and expressing the result in the time and frequency domain

$$\begin{aligned} P_a &= \frac{1}{\rho_0 c} \int_S \overline{p(t, \mathbf{r})^2} dS \\ &= \frac{1}{\rho_0 c} \int_{-\infty}^{+\infty} S_{uu}(f) |H(f, \mathbf{r}_{ref})|^2 Q(f, \mathbf{r}_{ref}) S df \end{aligned} \quad (3)$$

using the specific acoustic impedance  $\rho_0 c$ , the transfer function  $H(f, \mathbf{r}_{ref})$  between terminal voltage  $u(t)$  and sound pressure  $p(t, \mathbf{r}_{ref})$  at the reference point  $\mathbf{r}_{ref}$  (usually on-axis at 1 m distance from the source) and the directivity factor

$$Q(f, \mathbf{r}_{ref}) = \frac{S |p(f, \mathbf{r}_{ref})|^2}{\int_S |p(f, \mathbf{r})|^2 dS} \quad (4)$$

which describes the ratio between the power radiated by a virtual source generating the same sound pressure  $p(f, \mathbf{r}_{ref})$  on the reference point at all points on a spherical surface  $S$  and the real power integrated over  $S$ .

The total efficiency in Eq. (1) can also be approximated by a more convenient integral expression

$$\eta \approx \frac{\int_{-\infty}^{+\infty} \eta(f) S_{uu}(f) df}{\int_{-\infty}^{+\infty} S_{uu}(f) df} \quad (5)$$

using a frequency dependent efficiency factor

$$\eta(f) = \frac{|H(f, \mathbf{r}_{ref})|^2 Q(f, \mathbf{r}_{ref}) S}{\rho_0 c \Re(\underline{Z}_E(f)^{-1})} 100\% \quad (6)$$

weighted by the auto power spectrum  $S_{uu}(f)$  of voltage  $u(t)$  at the loudspeaker terminals. The approximation error is negligible for broadband stimuli and vanishes for a single tone completely.

The frequency dependent efficiency factor  $\eta(f)$  corresponds with previous discourse on loudspeaker efficiency based on linear modeling valid in the small signal domain [20]-[23].

This concept can also be applied to larger amplitudes where nonlinearities inherent in the loudspeaker and other time variant properties due to heating, aging and other visco-elastic properties cause a dependency of the transfer function  $H(f, \mathbf{r}_{ref})$ , directivity factor  $Q(f)$  and impedance  $\underline{Z}_E(f)$  on the particular input signal  $u(t)$ . In other words, the frequency responses are used as effective parameters of a relatively simple (linear) model approximating a much more complex problem.

### 4 Voltage Sensitivity

Most power amplifiers provide a low output impedance, and the terminal voltage  $u(t)$  corresponds with the audio input signal. The voltage sensitivity defined as the sound pressure level

$$SPL_{u_{ref}, \mathbf{r}_{ref}}(f) = 20 \log \left( \left| \frac{H(f, \mathbf{r}_{ref})}{p_0} u_{ref} \right| \right) \quad (7)$$

in dB for given reference rms value of the input voltage such as  $u_{ref} = 1V_{rms}$  at a given reference point  $\mathbf{r}_{ref}$  using the reference sound pressure  $p_0 = 2 \cdot 10^{-5} Pa$ . It is necessary to introduce the voltage sensitivity as a frequency dependent characteristic because a smart loudspeaker system with extensive use of equalization and linearization puts demanding

requirements on the power amplifier to generate the output without limiting.

## 5 Moving Coil Loudspeaker

The further investigations are performed on an electro-dynamic transducer using a moving coil in a static magnetic field.

The electro-acoustic transfer function of this transducer type can be modelled at small displacement  $x \approx 0$  and at lower frequencies where the influence of the voice coil inductance is negligible by

$$H(f, \mathbf{r}_{ref}) = \frac{\rho_0 f S_D Bl(x=0)}{|r_{ref}| R_E Z_{MT}(f)} \quad (8)$$

with the total mechanical impedance

$$Z_{MT}(\omega) = \frac{Bl(0)^2}{R_E} + R_{MS} + j\omega M_{MS} + \frac{K_{MT}(0)}{j\omega} \quad (9)$$

using the density of air  $\rho_0$ , the effective radiation area  $S_D$ , the nonlinear force factor  $Bl(x)$  characteristic, the DC resistance  $R_E$ , the mechanical resistance  $R_{MS}$  considering suspension and air losses, the total moving mass  $M_{MS}$  and the nonlinear stiffness characteristic  $K_{MT}(x)$  of the suspension and air in a sealed enclosure.

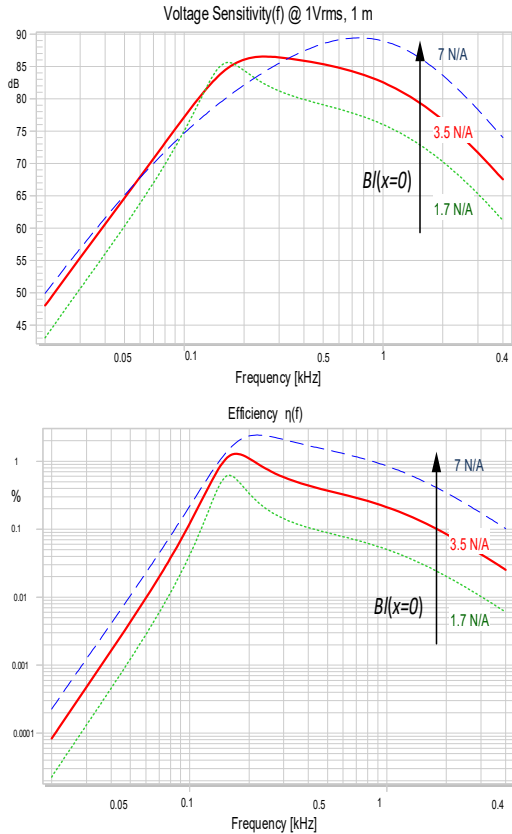


Figure 2: Efficiency  $\eta(f)$  and voltage sensitivity  $SPL_{1V,1m}(f)$  of an electro-dynamical loudspeaker mounted in a sealed enclosure (speaker **B**) versus frequency  $f$  of a single tone stimulus, using three different values of the force factor  $Bl(x=0)$  at the rest position.

Figure 2 shows the efficiency  $\eta(f)$  and voltage sensitivity  $SPL_{1V,1m}(f)$  of an electro-dynamical

loudspeaker mounted in a sealed enclosure calculated based on the lumped parameter model in Eqs. (8) and (9) assuming omnidirectional radiation into the half space for a sinusoidal tone of frequency  $f$ .

### 5.1 Passband Performance

The efficiency  $\eta(f)$  is almost constant in the passband of the loudspeaker with  $2f_s < f < 5f_s$ , where the back EMF is not active and the effect of the inductance and radiation load is negligible. This constant value is defined in standards (e.g. [12]) as reference efficiency  $\eta_0$  and can be described by the following lumped parameters based on linear modelling radiating into the half-space:

$$\eta_0 = \frac{Bl(0)^2}{R_E M_{MS}^2} \frac{\rho S_D^2}{2\pi c} 100\% \quad (10)$$

The reference efficiency  $\eta_0$  rises with force factor  $Bl(x=0)$  and the effective radiation area  $S_D$ , but is inversely related to DC resistance  $R_E$  and moving mass  $M_{MS}$ .

At higher amplitudes, the force factor product  $Bl$  is not a constant but becomes a nonlinear function  $Bl(x)$  depending on voice coil displacement  $x$ . Considering the probability density function  $pdf(x)$  of the displacement, the effective force factor can be calculated

$$\overline{Bl} = \int_{-\infty}^{\infty} Bl(x) pdf(x) dx \quad (11)$$

which can replace the force factor value  $Bl(x=0)$  at rest position in (10).

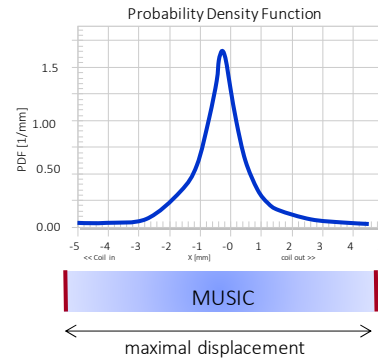


Figure 3: Probability Density Function  $pdf(x)$  of voice coil displacement  $x$  for a typical audio signals (e.g. music)

Figure 3 shows an example of the  $pdf(x)$  of typical audio material representing most music genres and speech. This bell-shaped characteristic shows that the coil is close to the rest position most of the time, and high peak values are relatively rare. Thus, from a statistical perspective the effective force factor  $\overline{Bl}$  is close to the force factor  $Bl(0)$  at the rest position  $x=0$ . This is an important discovery, that passband efficiency in the large signal domain is similar to the reference efficiency  $\eta_0$  calculated by linear modelling.

The reference efficiency  $\eta_0$  is directly related to the reference sensitivity defined in the pass band as

$$\begin{aligned} SPL_{1W,1m}(f) &= 10 \log \left( \left| \frac{H(f, \mathbf{r}_{ref})}{p_0} \right|^2 \frac{Z_N 1W}{p_0} \right) \\ &= 10 \log \left( \frac{\eta_0 1W}{100\% \Pi_0} \frac{Z_N}{R_E} \right) - 8dB \quad (12) \\ &= 10 \log \left( \frac{\eta_0}{100\%} \frac{Z_N}{R_E} \right) + 112dB \end{aligned}$$

with the standard reference power  $\Pi_0=10^{-12}$  W. The reference sensitivity is actually a voltage sensitivity but refers to the input power of 1 W considering the nominal impedance  $Z_N$  that is a frequency independent value rated by the manufacturer (usually 4 or 8 Ohm). Thus, the reference sensitivity in Eq. (12) can be measured with a constant terminal voltage (usually 2 or 2.8 Vrms) depending on the nominal impedance  $Z_N$  of the device under test. For defining the peak voltage requirement of the amplifier and selecting the transducer with optimum nominal input impedance  $Z_N$ , it is more convenient to use the voltage sensitivity as defined in Eq. (7) with a constant reference voltage (e.g.  $u_{ref}=1V_{rms}$ ).

## 5.2 Fundamental Resonance

The efficiency of the loudspeaker at the fundamental resonance frequency  $f_s$  can be calculated by

$$\eta(f_s) = \frac{\overline{Bl}^2 S_D^2 \rho_0 2\pi f_s^2}{(\overline{Bl}^2 + R_E R_{MS}) R_{MS} c} \quad (13)$$

In woofers and other transducers, where the electrical resistance transformed to the mechanical domain  $\overline{Bl}^2 / R_E$  is much larger than the mechanical resistance  $R_{MS}$  and the electrical damping dominates the total damping, the efficiency  $\eta(f_s)$  is described as

$$\eta(f_s) = \frac{S_D^2 \rho_0 2\pi f_s^2}{R_{MS} c} \quad (14)$$

and becomes independent of force factor  $\overline{Bl}$  and DC resistance  $R_E$ . The small value of the mechanical resistance  $R_{MS}$  generates a distinct maximum of the efficiency at resonance ( $\eta(f_s) > \eta_0$ ). However, a high force factor value  $Bl(0)$  will reduce the voltage sensitivity at the resonance to

$$SPL_{u_{ref}, f_{ref}}(f_s) = 20 \log \left( \frac{\rho_0 f_s S_D}{r_{ref}} \frac{u_{ref}}{|Bl(0)| p_0} \right) \quad (15)$$

Contrary to the passband region where efficiency and voltage sensitivity are rising with the force factor, a low force factor  $Bl(0)$  would improve the voltage sensitivity at resonance. That means, a subwoofer designed for a narrow audio band close to the fundamental resonance can use a weak motor with a small force factor  $Bl(0)$  but would be the best choice for high efficiency and high voltage sensitivity [21]. However, the volume of the enclosure and other geometrical constraints require to operate the loudspeaker in many applications also at frequencies below the first fundamental resonance.

## 5.3 Low Frequencies

A transducer mounted in a sealed enclosure generates, at low frequencies  $f < f_s/2$ , the efficiency

$$\eta(f) = (2\pi f)^2 \frac{\overline{Bl}^2 \rho S_D^2}{R_E \overline{K_T}^2 2\pi c} \quad (16)$$

using the effective force factor  $\overline{Bl}$  considering the  $pdf(x)$  of the voice coil displacement  $x$  according Eq. (11) and the effective total stiffness

$$\overline{K_T} = \int_{-\infty}^{\infty} (K_{MS}(x) + K_{MB}(x)) pdf(x) dx \quad (17)$$

calculated by the nonlinear stiffness characteristics  $K_{MS}(x)$  and  $K_{MB}(x)$  of the mechanical suspension and air volume, respectively.

## 6 Maximizing Efficiency

After presenting the fundamental relationships between efficiency and lumped transducer parameters, this section discusses the influence of the geometry, choice of the material and other design parameters.

### 6.1 Gap-Coil Topology

For an electro-dynamical transducer, the relationship between the gap depth  $h_g$  and the voice coil height  $h_c$  is a good starting point in our search for maximum efficiency in sound reproduction.

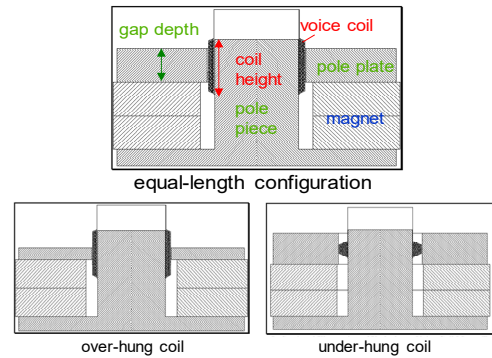


Figure 4: Common topologies for configuring the gap-depth and voice coil height in electro-dynamical transducers

Figure 4 shows typical configurations to maximize either efficiency or linearity of the electro-dynamical transducer. The so-called equal-length configuration uses a minimum voice coil overhang to exploit the magnetic fringe field outside the gap. This configuration gives the highest force factor value  $Bl(x=0)$  at the voice coil rest position, which is beneficial for maximizing the effective force factor  $\overline{Bl}$  when reproducing common audio signals. Unfortunately, this configuration generates significant harmonic and intermodulation distortion and other undesired nonlinear symptoms (DC-displacement, instabilities,...) for voice coil displacement  $x$ . For example, Figure 5 shows the nonlinear force factor characteristic  $Bl(x)$  calculated by a magnetic FE model where the gap depth  $h_g$  was varied between 5, 10, 15 and 20 mm while assuming

the coil height  $h_c=10$  mm and magnet size are constant [17].

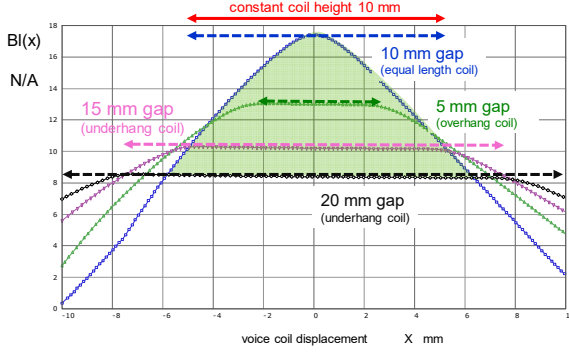


Figure 5: Force factor  $Bl(x)$  versus displacement  $x$  of an equal-length, an overhang and under-hang configurations.

The overhang configuration shown in Figure 4 uses spare windings below and above the gap, waiting to be used when the voice coil is moved. This generates a plateau in the  $Bl(x)$  characteristic in Figure 5, giving more linearity and less nonlinear distortion for moderate excursion.

The underhang configuration in Figure 4 uses wider pole plates and a short coil to generate a linear plateau in the nonlinear  $Bl(x)$  characteristics and creates more linearity.

The price paid for less  $Bl(x)$ -variation and lower nonlinear distortion is a loss of force factor, illustrated as shadowed area in Figure 5.

Topology	Equal-length	Over-hang	Under-hang
Motor efficiency factor $\overline{Bl}^2 / R_E$	high	low	low
Moving mass $M_{MS}$	medium	high	low
$Bl(x)$ -nonlinearity	strong	weak	weak
$L(x)$ -nonlinearity	medium	strong	weak
DC-Stability	critical	robust	robust
Weight, size cost	low	medium	high

Table 1: Overview on benefits and drawbacks of selected motor topologies using different ratios between voice coil height and depth length

Table 1 summarizes the properties of the common motor topologies. The equal-length configuration has been used for consumer applications where maximum output, efficiency, cost, size and weight requires a compromise with linearity. The overhang configuration is attractive for subwoofer applications where the moving mass and inductance nonlinearities  $L(x)$  and  $L(i)$  are less important. The underhang coil is an interesting topology for all high-frequency applications (e.g. tweeter) where the coil mass limits the overall efficiency. While, both the overhang and underhang configurations are relatively robust to an offset of the voice coil rest position caused by production variances and aging, the equal-length configuration reacts very sensitive

to an offset and may generate a significant DC displacement by rectifying the AC audio signal.

Nevertheless, the equal-length configuration has the highest potential for active systems where the passive transducer provides the highest efficiency over a wide audio band and digital signal processing can be used to cancel the nonlinear loudspeaker distortion and actively stabilize the voice coil position. For this reason, the remaining parts of this section focus on the optimal design of the equal-length configuration.

## 6.2 Motor Efficiency Factor

The efficiency at low frequencies and in the passband in Eqs. (10) and (16) depends on the squared effective force factor divided by the DC resistance, which can be interpreted as a motor efficiency factor  $\overline{Bl}^2 / R_E$ .

Expressing DC resistance as

$$R_E = \rho_E \frac{l}{A_w} = \rho_E \frac{l^2}{V_w} \quad (18)$$

and neglecting the magnetic fringe field outside the gap allows the motor efficiency factor to be written as

$$\frac{\overline{Bl}^2}{R_E} = \overline{B}^2 \frac{V_w}{\rho_E} \quad (19)$$

using  $\overline{B}^2$  to represent the mean induction seen by the conductive wire material of the volume  $V_w$  and the electrical resistivity  $\rho_E$ . The volume  $V_w$  can be increased by maximizing the fill factor in the coil winding area [18] by using rectangular wire and an efficient winding layout, which usually increases the manufacturing effort and cost. In practice, there is not much freedom to increase volume  $V_w$  by using a thinner bobbin material and reducing the clearance in the gap, which is required to cope with rocking modes and voice coil rubbing. However, the motor efficiency factor  $\overline{Bl}^2 / R_E$  is independent of the wire length  $l$  and cross-sectional area  $A_w$  of the wire. This fact gives the loudspeaker designer some freedom in trading force factor against DC resistance and realizing a desired voltage sensitivity, as discussed below in section 7.

## 6.3 Coil Material

The electrical resistivity  $\rho_E$  and the density  $\rho_D$  of the wire material affect the DC resistance  $R_E$  and the total moving mass  $M_{MS}$ , respectively. This has a significant influence on the pass band efficiency

$$\eta_0 = \frac{\overline{B}^2 V_w \rho_0 S_D^2}{\rho_E (\rho_D V_w + M_{add})^2 2\pi c} \quad (20)$$

considering the additional mass  $M_{add}$  representing the contribution of other moving loudspeaker parts such as suspension, diaphragm and bobbin.

Choosing the volume  $V_w$  and the proper material of the wire depend on the ratio between additional mass and coil mass:



$$M_{ratio} = \frac{M_{add}}{\rho_D V_w} \quad (21)$$

If the mass ratio  $M_{ratio} \gg 1$ , a larger wire volume  $V_w$  increases the pass band efficiency. Using an aluminum coil instead of copper would reduce the passband efficiency  $\eta_0$  by half if the coil mass is negligible compared to the total mass  $M_{MS}$  because aluminum has a higher resistivity. If the mass ratio  $M_{ratio} \ll 1$  and the coil mass dominates the total moving mass  $M_{MS}$ , an aluminum coil provides 6 times more passband efficiency than a copper coil.

#### 6.4 Voice Coil Height

The voice coil height  $h_c$  limits the maximum displacement  $X_{max}$  in an equal-length configuration. The IEC standard [13] defines peak displacement limited by the  $Bl(x)$ -nonlinearity by the maximum excursion where the  $Bl(x)$  drops to 82 % of the force factor value  $Bl(x=0)$  at the rest position. This definition corresponds to 10% intermodulation distortion generated by a two-tone signal [24]. If nonlinear control can be applied to the loudspeaker and the nonlinear distortion can be cancelled actively, the maximum displacement can be increased to half of the voice coil height ( $X_{max} = h_c/2$ ), where the force factor decreases to half of the  $Bl$  found at the rest position

$$Bl\left(x = \pm \frac{h_c}{2}\right) \approx 0.5Bl(x=0) \quad (22)$$

Theoretically, the nonlinear control can be applied to larger peak displacements, but the compensation of the  $Bl(x)$  would increase significantly the peak voltage requirements applied to the power amplifier. Exploiting the  $Bl(x)$  down to the 50% point is a good compromise for active linearization of a loudspeaker reproducing common (broadband) audio signals with a probability density function  $pdf(x)$  as shown in Figure 3. In this case there is no increase in power consumption and only a moderate increase in peak voltage requirement.

#### 6.5 Gap depth

After defining the voice coil height  $h_c$ , the optimal gap depth  $h_g$  shall be determined to exploit the magnetic fringe field outside the gap. The induction  $B$  within the gap and in the fringe field, as illustrated in Figure 6, can be calculated by using a magnetic finite element simulation tool.

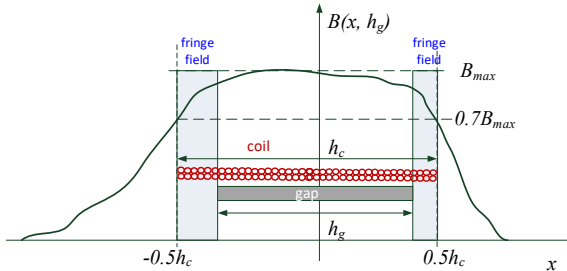


Figure 6: Exploiting the magnetic fringe field in the magnetic induction  $B(x, h_g)$  outside the magnetic gap with the gap depth  $h_g$  by the voice coil overhang.

The optimal value  $h_g$  can be found by finding a gap geometry at which the induction at both ends of the voice coil

$$B(x = \pm 0.5h_c, h_g) = 0.7B_{max} \quad (23)$$

is 70% of the maximum induction  $B_{max}$  in the gap. For a smaller value of the gap depth  $h_g$ , the windings at both ends of the voice coil would generate a lower contribution to the squared  $Bl$  value while increasing the electrical resistance  $R_E$ , giving a lower motor efficiency factor  $Bl^2/R_E$ .

#### 6.6 Magnet Geometry

After defining the clearance between the voice coil and the pole plates, the gap width  $w_g$  and the pole plate surface  $A_g$  can be determined, giving the gap volume  $V_g = A_g w_g$ . In order to generate the highest induction  $B_g$  in the gap, the optimal working point in the demagnetization curve shown in Figure 7 must be used.

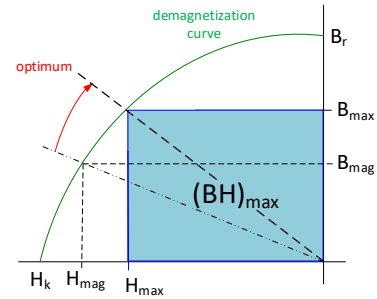


Figure 7: Optimal working point in the demagnetization curve of the magnet.

The induction  $B_{mag}$  and field strength  $H_{mag}$  in the magnet should be close to the optimal values  $B_{max}$  and  $H_{max}$ , giving the maximum product

$$\text{Max}(B_{mag} H_{mag}) = B_{max} H_{max} = (BH)_{max} \quad (24)$$

with maximum energy product  $(BH)_{max}$ , which is an important material parameter of the magnet.

Neglecting the iron in the pole piece and plates, the maximum value of the induction in the gap for a given magnet volume  $V_m = h_m A_m$  can be estimated by

$$B_g = \sqrt{\frac{\mu_0 (BH)_{max} V_m}{V_g}} \quad (25)$$

This value can be realized if magnet height

$$h_m = \frac{B_g w_g}{\mu_0 H_{max}} \quad (26)$$

and cross-sectional area

$$A_m = \frac{B_g A_g}{B_{max}} \quad (27)$$

corresponds to the gap width  $w_g$  and the pole plate surface  $A_g$  of the gap. Modern FE magnetic simulation tools simplify this optimization process while considering the saturation of the iron material and the fringe field outside the gap.

## 6.7 Suspension

The total stiffness  $K_{MT}$  is the critical parameter in the denominator in Eq. (16) that reduces the efficiency at low frequency. If the transducer has a relatively large radiation area  $S_D$  and is operated in a relatively small enclosure of volume  $V_{AB}$ , the stiffness  $K_{MB}$  representing the air compression is much larger than the mechanical stiffness  $K_{MS}$  and limits the efficiency at low frequencies:

$$\eta(f) \approx (2\pi f)^4 \frac{\rho_0 (\overline{Bl})^2 V_{AB}^2}{2\pi c R_E (p_0 \kappa)^2 S_D^2} \quad (28)$$

It is interesting to note that a lower effective radiation area  $S_D$  would increase the efficiency at low frequencies, but this would reduce the efficiency at higher frequencies. It is more beneficial to fill the volume with a porous absorbing material (e.g. charcoal) to bypass the acoustical stiffness by a resistive element, effectively increasing the volume size of the box.

In practice, the enclosure is only sealed for frequencies in the audio band but is provided with a small barometric vent to ensure the air exchange for static pressure differences to the ambience. Thus, the acoustical spring vanishes at low frequencies, and only the mechanical suspension keeps the coil at the optimal rest position. This is very important for the equal-length configuration, where a small coil offset leads to a significant asymmetry in the  $Bl(x)$ -nonlinearity. External forces generated by gravity and static air pressure differences on the front and rear side of a diaphragm in automotive applications may also change the voice coil position. A DC force generated dynamically by the nonlinear rectification process only works against the mechanical stiffness  $K_{MS}(x=0)$ . If the mechanical suspension is too soft, a static offset and dynamic DC displacement might be generated, leading to bifurcation, other unstable behavior and excessive distortion. Furthermore, a mechanical suspension that is still stiff enough after break-in becomes softer later in product life due to fatigue in the rubber, fabric, foam and suspension materials and at particular climate conditions. Mechanical overload may also speed up the natural aging process. Adaptive nonlinear control can cope with unreliable mechanical suspension. Active stabilization and linearization keeps the voice coil at the optimal voice coil rest position and ensures maximum AC displacement and sound pressure output. The active protection system prevents an overload of the transducer and provides more reliability than the self-protection capabilities provided by the transducer itself.

Thus, the new DSP functionality allows for the transversal stiffness generated by spider and surround to be reduced, giving more efficiency at low frequencies and requiring less peak voltage to move the coil to the target displacement.

However, the mechanical suspension is still the most critical part in loudspeaker design and manufacturing. The new degrees of freedom provided by DSP have to be used to ensure sufficient rotational stiffness of the coil against tilting, giving

robustness against rocking modes generated by imbalances in the mass, stiffness and force factor distribution in the gap [25]. This is important for flat loudspeakers where the distance between spider and surround is small, or in headphones, micro-speakers, compression drivers and other transducers where no spider is used.

The surround is clearly the most critical part in loudspeakers, because voice coil displacement and air pressure in the rear enclosure generate significant deformation which affects also the modal vibration at higher frequencies.

## 7 Optimizing Voltage Sensitivity

The voltage sensitivity of the transducer in Eq. (7) is a useful characteristic to decide whether the peak voltage capabilities of the power amplifier are sufficient to generate the target SPL output at all frequencies of interest.

It is possible to modify the voltage sensitivity without significantly degrading the efficiency, which was the primary design goal so far. For example, changing the DC resistance  $R_E$  of the voice coil while maintaining the same motor efficiency factor  $\overline{Bl}^2 / R_E$  will not change the efficiency  $\eta(f)$  in Eqs. (10), (13) and (16) as long as the Volume  $V_C$  of the wire material is constant. Since the transfer function in Eq. (8) is inversely proportional to the square root of  $R_E$ , assuming a constant motor efficiency factor  $\overline{Bl}^2 / R_E$ , the difference in the voltage sensitivity of two designs with only different DC resistances  $R_E$  and  $R_E'$  becomes:

$$\begin{aligned} & SPL_{V,1m}(f) \Big|_{R_E} - SPL_{V,1m}(f) \Big|_{R_E'} \\ &= 10 \log \left( \frac{R_E'}{R_E} \right) \end{aligned} \quad (29)$$

Surprisingly, this is also valid for the resonance frequency  $f_s$  because the constant motor efficiency factor appears as the electric damping in Eq. (9). Practically speaking, reducing the DC resistance to half of its value gives 3dB more voltage sensitivity.

Passive Loudspeaker	A	B	Change
Nominal Impedance [ $\Omega$ ]	4	2	
Gap depth $d_g$ [mm]	5	5	
Coil Height $h_c$ [mm]	11	5.75	
Resistance $R_E$ [ $\Omega$ ]	3.3	1.75	-47%
Force factor $Bl(0)$ [N/A]	4.4	3.4	-23%
Motor efficiency factor $Bl(0)^2/R_E$ [Ns/m]	5.86	6.6	+13%
Compliance $C_{ms}$ [mm/N]	0.134	0.137	
Moving mass $M_{MS}$ [g]	9.92	8.0	-19%
Mass ratio $M_{ratio}$	1.5	3	
Resonance frequency $f_s$ [Hz]	138	152	

Pass Band Efficiency $\eta_0$ [%]	0.23	0.38	<b>+65%</b>
Reference (power) sensitivity in passband $SPL_{1W,1m}$ [dB]	86.6	88.6	<b>+2.0dB</b>
Voltage sensitivity in passband $SPL_{1Vrms,1m}$ [dB]	80.1	85.1	<b>+5.0dB</b>

Table 2: Characteristics of the original transducer (A) and the optimized transducer (B) with reduced voice coil height  $h_c$ .

## 8 Case Study

The new degrees of freedom provided by nonlinear adaptive control shall be illustrated on an existing 4.5" woofer **A** developed for automotive applications. A minor modification has been performed in transducer **B** by shorting the voice coil to half of the height found in the original transducer **A** while using the same coil wire, magnetic system, suspension and diaphragm. This change has not increased the cost and could be accomplished without redesigning the motor structure. Although the modified transducer **B** has not been optimized to the maximum efficiency this small modification improves the total performance of the transducer with nonlinear control significantly.

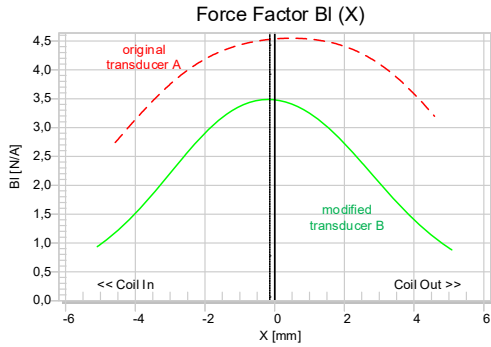


Figure 8: Force factor characteristic  $Bl(x)$  of an equal-length and an overhang configuration

### 8.1 Loudspeaker Parameters

Figure 8 shows that the original transducer **A** with voice coil overhang of 6 mm does not have a linear plateau region where the force factor  $Bl(x)$  is constant for small displacement  $|x| < 3$  mm. A significant fringe field outside the gap generates this nonlinearity but also gives 23% more force factor  $Bl(x=0)$  at the rest position than the modified speaker **B** with the shorter coil height  $h_c \approx h_g$ . However, the reduced DC resistance  $R_E = 1.75\Omega$  leads to a 13% higher motor efficiency factor  $Bl^2/R_E$  in the modified speaker **B**. The same improvement can be measured in the total efficiency  $\eta(f < f_s)$  below resonance. The motor efficiency factor can be further optimized by a slightly longer coil  $h_c \approx 7$  mm to exploit the fringe field according to the condition specified in Eq. (26). A motor design tool based on magnet FE analysis can be used to find the optimal voice and wire dimensions giving the nominal impedance of 2  $\Omega$ .

The shorter coil in the modified transducer **B** reduces the total moving mass  $M_{MS}$  by 19 %. This shifts the resonance frequency  $f_s$  slightly up because the total stiffness nearly stays constant due to the small air volume in the sealed box. Since the mass ratio  $M_{ratio}$  is close to 1, the reduction of the voice coil mass has still a large influence on the pass band efficiency. According to Eq. (10), the total pass-band efficiency  $\eta_0$  is increased by 65 %, corresponding with an increase of 2 dB more reference passband sensitivity  $SPL_{1W,1m}(f > f_s)$  considering 1W nominal input power. The voltage sensitivity  $SPL_{1Vrms,1m}(f > f_s)$ , which is required to determine the peak voltage demands of the amplifier, is 5dB higher because the modified loudspeaker has only half of the nominal input impedance  $Z_n$ .

Active Speaker	A+LC	B+LC	A+NC	B+NC
$SPL$ [dB]	91.8	92.1	92.2	92.2
Displacement peak $X_p$ [mm]	3.3	3.4	3.2	3.3
Displacement rms $X_{ac}$ [mm]	0.51	0.53	0.51	0.54
Crest factor $C_X$ [dB]	16.1	16.1	15.9	15.9
Distortion $EID$ [%]	-	-	11	30 (+19%)
Voltage peak $U_p$ [V]	45.5	26.8	45.6	30.4 (-33%)
Voltage rms $U_{ac}$ [V <sub>rms</sub> ]	8.7	4.7	8.7	4.7 (-45%)
Crest factor $C_u$ [dB]	14.3	15.1	14.3	16.2
Real input power $P_e$ [W]			14.2	8.4 (-40%)
Temperature coil $\Delta T_v$ [K]			+96K	+59K (-39%)

Table 3: Performance of the original loudspeaker (A) and the modified speaker (B) with linear control (+LC) and nonlinear control (+NC) while reproducing a typical audio signal.

### 8.2 Audio Reproduction

Table 3 shows the performance of the original (A) and modified transducer (B) mounted in a 1.6 liter sealed enclosure operated with linear control (+LC) and with nonlinear control (+NC) while reproducing a typical audio stimulus (*Tracy Chapman, Crossroads, This Time*) low-pass filtered at 1.5 kHz crossover frequency. Both the linear and the nonlinear control techniques have been realized by the KCS-technology [27] based on voltage and current monitoring and implemented in a micro-controller ARM M4. Only the nonlinear controller stabilizes the voice coil position, compensates for nonlinear distortion and generates a linear relationship between control input and sound pressure output. Different equalization applied to



each speaker generates the same 6<sup>th</sup>-order Chebyshev alignment at a cutoff frequency  $f_c=100\text{Hz}$ . The linear control cannot cope with the compression, DC displacement and other nonlinear effects at higher amplitudes.

The magnitude of music stimulus is adjusted at the control input of all four active loudspeaker systems listed in Table 3 to produce a total SPL  $\approx 92\text{ dB}$  at a distance of  $r=0,1\text{m}$ . The nonlinear control system also provides reliable mechanical and thermal protection systems and attenuates the input signal if the peak displacement would exceed  $x_{prot}=3.5\text{ mm}$  or if the voice coil temperature would rise more than  $\Delta T_{prot}=130\text{ K}$ . The linear control would larger safety margin in the mechanical protection due to the uncertainties in the voice coil position.

The four active speakers generate similar sound pressure spectra, almost the same rms and peak displacement giving a crest factor  $C_x$  of the 16 dB, which is typical for common audio signals. Thus, most of the time the coil stays in the gap, and the effective force factor is nearly equal to the maximum  $Bl(x=0)$  at the rest position.

The nonlinear control system for the linearization of the original speaker (**A+NC**) needs low compensation distortions EID that are 11 % of the peak value of the terminal voltage and do not change the crest factor  $C_u=14.3\text{ dB}$  of the input signal. The linearization of the modified speaker (**B+NC**) requires three times more peak value of the compensation distortion which increases the crest factor by about 1 dB compared with linear control (**B+LC**). However, this increase is similar to the effect of the equalization at low frequencies. The different alignment of original and modified speaker (**A+LC**) and (**B+LC**) generates an increase of the crest factor in the terminal voltage by 0.5 dB and 1.3 dB, respectively, due to the difference in the resonance frequency  $f_s$ . This increase is caused by boosting low frequency components having a higher crest factor ( $C_x\approx 16\text{dB}$ ) than the full band audio signal.

This small increase in the crest factor can be easily compensated by the much better voltage sensitivity of the modified speaker with nonlinear control **B+NC** compared the original speaker **A+NC**, which reduces the peak voltage requirement for the amplifier by 33 %.

The shorter coil in the modified speaker reduces the power consumption and the heat development under nonlinear control **B+NC** by 40%. This transducer operated with reliable active protection (**B+NC**) can generate at least 3 dB more SPL (measured as a total mean value over the stimulus) by requiring less peak voltage as in the original speaker **A+NC**. Exploiting the full voltage capability provided by the amplifier, the mechanical protection system in the modified speaker **B+NC** would be activated and would reduce the bass signal ( $f < f_s$ ) by -3dB to keep the peak excursion below  $x_{prot}=3.5\text{ mm}$ . The 3dB increase of SPL would require 17 W of real input power and would heat up the voice coil temperature by  $\Delta T_v\approx 120\text{ Kelvin}$  what would be permissible for the

speaker. Doubling the electric input power provided to the original speaker **A** would not only require a more powerful amplifier but would also generate an unacceptable increase of the coil temperature  $\Delta T_v\approx 200\text{ Kelvin}$ .

### 8.3 Distortion Reduction

Figure 9 shows the active compensation of the harmonic distortion generated by a single excitation tone. Since the modified transducer **B** is carefully manufactured, the 2<sup>nd</sup>-order distortion found under linear control is relatively small, indicating an optimal voice coil rest position and a symmetrical stiffness characteristic. The nonlinear control **NC** is required for speaker **B** to reduce the high value (40 %) of 3<sup>rd</sup>-order harmonic distortion by 20 dB at low frequencies.

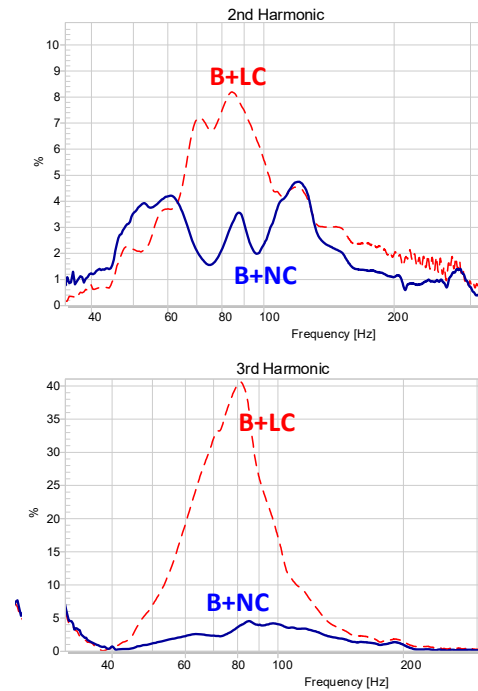


Figure 9: 2<sup>nd</sup>- and 3<sup>rd</sup> order harmonic distortion of the optimized loudspeaker with linear control (**B+LC**) and nonlinear control (**B+NC**).

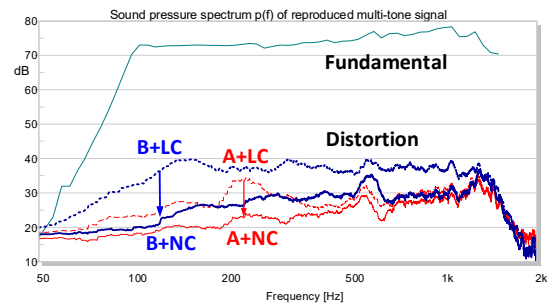


Figure 10: Fundamental components and nonlinear distortion in a multi-tone test stimulus reproduced by the original loudspeaker (**A**) and the modified loudspeaker (**B**) with linear (+LC) and nonlinear control (+NC).

The active cancelation of intermodulation distortion can be easily checked by reproducing a multi-tone stimulus where the nonlinear distortion components can easily be separated from the sparse fundamental components supplied by the stimulus. The distortion cancellation applied to the original speaker **A+NC** and modified speaker **B+NC** are shown as thin solid and thick solid lines in Figure 10, respectively, while the dashed lines represent the nonlinear distortion found with linear control **LC**. The modified speaker with linear control **B+LC** generates much higher distortion than the original speaker **A+LC** but nonlinear control can reduce the distortion by more than 15 dB at low frequencies. Here the nonlinear motor with nonlinear control **B+NC** generates lower distortion than the original speaker **A+LC** that uses a much more linear motor. At 600 Hz and 1.3 kHz there are nonlinear modal vibrations which cannot be canceled by the current control structure based on lumped parameter modeling.

## 9 Consequences for the Amplifier

The high crest factor ( $C_u > 12$  dB) of common audio signals makes the peak voltage to a more limiting factor in amplifiers than the long-term power capabilities. This becomes even worse in efficient transducers having a high motor efficiency factor  $\overline{Bl}^2 / R_E$  that increases the electric damping, giving a low-quality factor (e.g.  $Q_{TS} < 0.3$  in woofers) and low voltage sensitivity at the resonance frequency  $f_s$ . Reducing the DC resistance  $R_E$  of the coil, as suggested in section 7, is a practical solution but requires short cables and a low output impedance of the power amplifier. Placing the power amplification closer to transducer or even integrating both components in one active module will not only solve the cable problems but allows for simplification of the output filter in Class D amplifiers while fulfilling the EMC requirements. However, reducing the DC resistance  $R_E$  will increase the current and the heat development in the amplifier output stage. Even if the amplifier can provide the rms current and long-term power to the speaker, the high crest factor of common audio signals generates high current peaks which may lead to a critical temperature in the amplifier output stage after a short thermal time constant. A smart protection system for amplifiers would provide maximum peak currents and would attenuate the audio signal temporarily if the monitored temperature approaches a critical value. Thus, the thermal protection of the amplifier is a very similar problem to the thermal protection of the voice coil in the transducer, although there are significant differences in the heat flow, the cooling mechanisms and the thermal time constants. Combining the protection of both FET output stage and coil in a common control block would improve the maximum short-term power capacity of the amplifier.

## 10 Conclusions

Feeding the current and voltage signal back to the DSP leads to an adaptive control architecture that generates a desired linear transfer behavior over the life time of the loudspeaker system while coping with production variances, transducer nonlinearities, overloading, fatigue, aging, climate and other external disturbances. Thus, software algorithms can complement the hardware design giving a superior overall system. For example, a nonlinear transducer combined with nonlinear distortion cancelation provides better sound quality, more efficiency and lower cost than conventional passive solutions. Maximizing total efficiency for a typical audio signal has the highest priority in loudspeaker design, as illustrated in an electro-dynamical transducer in this paper. This analysis can be continued for the design of an optimal control system driving one or more transducers placed on a complex mechanical structure (e.g. panel) to generate a desired 3D sound field. Maximizing efficiency should be also the first criterion in optimizing modal vibration, acoustical radiation and the optimal placement of the radiators. The total efficiency can also be estimated for reproducing any audio signals at small and high amplitudes if the spectral properties and amplitude distribution of the stimulus are known.

The voltage sensitivity is a second important transducer characteristic which is required to estimate the peak voltage and peak current that has to be provided by the power amplifier, considering the high crest factor  $C_u$  of common audio signals. The capability of the amplifier to generate a high value of short term power for a limited time (a few milliseconds) becomes more important in efficient loudspeakers where the long-term power consumption will be reduced. The voltage sensitivity of the transducer can be adjusted to the amplifier capabilities while sustaining the maximum efficiency of the transducer. Thus, a closer integration of transduction, amplification and digital signal processing in one active transducer module provides further potential for improving the performance-cost ratio of loudspeakers.

## 11 References

- [1] G. Ramos, J. Lopez, "Filter Design Method for Loudspeaker Equalization Based on IIR Parametric Filters," J. Audio Eng. Soc., Vol. 54, No. 12 pp. 1162-1178; December 2006.
- [2] G. Vignon and S. Scarlett, "Specifying Xmax for Micro-speakers and Smart Amplifiers", presented at the 137<sup>th</sup> Convention of the Audio Eng. Soc. 2014, Oct. 9-12<sup>th</sup>, Los Angeles, USA, preprint 9114.
- [3] W. Klippel, "Mechanical Overload Protection of Loudspeaker Systems," J. Audio Eng. Soc., Vol. 64, No. 10, October 2016, pp. 771 – 783.
- [4] W. Klippel, "Loudspeaker Nonlinearities – Causes Parameters, Symptoms," J. Audio Eng. Soc. 54, no. 10, pp 907 – 939 (oct. 2006).
- [5] W. Klippel, "The Mirror Filter - a New Basis for Reducing Nonlinear Distortion Reduction and

- Equalizing Response in Woofer Systems", *J. Audio Eng. Society* 32, Heft 9, S. 675-691, (1992).
- [6] W. Klippel, "Adaptive Nonlinear Control of Loudspeaker Systems," *J. Audio Eng. Society* 46, pp. 939 - 954 (1998).
- [7] W. Klippel, „Active Compensation of Transducer Nonlinearities," preprint in 23rd International Conference of the *Audio Eng. Society* on "Signal Processing in Audio Recording and Reproduction", Copenhagen, Denmark, 23-25 May 2003.
- [8] W. Klippel, "Adaptive Stabilization of Electrodynamic Transducers", *J. Audio Eng. Soc.* Vol. 63, No. 3 pp. 154-160; March 2015.
- [9] L. Beranek, T. Mellow, "Acoustics: Sound Field and Transducers," Academic Press, Amsterdam, 2012
- [10] R. Small, "Direct Radiator Loudspeaker System Analysis," *J. Audio Eng. Soc.* 1972, Vol. 20, No. 5, pp. 307-327.
- [11] IEC 60268-21: Sound System Equipment – Part Acoustical (Output Based) Measurements, draft 2017
- [12] IEC 60268-22: (Draft) Sound System Equipment – Electrical and Mechanical Measurements on Transducers, draft 2017
- [13] IEC 62458:2010 Sound System Equipment – Electro-acoustical Transducers – Measurement of Large Signal Parameters
- [14] Audio Engineering Society, "AES20-1996: AES recommended practice for professional audio - subjective evaluation of loudspeakers (reaffirmed 2007)", *J. Audio Eng. Soc.* 44(5), 382-400 (1996)
- [15] W. Klippel, "Mechanical Fatigue and Load-Induced Aging of Loudspeaker Suspension," presented at the 131<sup>st</sup> Convention of Audio Eng. Soc. 2011, Oct. 20-23, NY, USA
- [16] F. Agerkvist and B. R. Pedersen, "Time varying behaviour of the loudspeaker suspension: Displacement level dependency," presented at the 127th Convention of the Audio Engineering Society, New York, (7902), October 2009.
- [17] M. Dodd, personal communication.
- [18] N. E. Iversen, et. al. "Relationship between Voice Coil Fill Factor and Loudspeaker Efficiency," *JAES* Volume 64 Issue 4 pp. 241-252; April 2016.
- [19] W. M. Leach, "Introduction to Electroacoustics and Audio Amplifier Design", Kendall/Hunt Publishing Company, 2003.
- [20] J. Vanderkooy, P. Boers, and R. Aarts, "Direct-Radiator Loudspeaker Systems with High Bl," *J. Audio Eng. Soc.*, vol. 51, no. 7/8 (July/August 2003).
- [21] R. Aarts, "High-efficiency low-Bl loudspeakers," *J. Audio Eng. Soc.* Vol. 53, pp. 579–592 (2005).
- [22] D. B. Keele, "Maximum Efficiency of Direct Radiator Loudspeakers," presented at the 91<sup>st</sup> Convention of the Audio Eng. Soc., preprint No. 3193 (Oct. 1991).
- [23] N. E. Iversen, A. Knott and M. A. E. Andersen, "Low Impedance Voice Coils for Improved Loudspeaker Efficiency", in AES Convention 139th, New York October 29th-1st November, 2015.
- [24] W. Klippel, "Assessment of Voice-Coil Peak Displacement X<sub>max</sub>", *J. Audio Eng. Soc.* Vol. 51, No. 5, pp. 307-324; May 2003.
- [25] W. Cardenas, W. Klippel, "Root Cause Analysis of Rocking Modes," *J. Audio Eng. Soc.*, Vol. 64, No. 12, pp. 969-977; December 2016
- [26] S. Poulsen and M. A. E. Andersen, "Practical considerations for integrating switch mode audio amplifiers and loudspeakers for a higher power efficiency", in AES Convention 116th, Berlin May 8-11, 2004.
- [27] Klippel Controlled Sound (KCS), Klippel GmbH, [www.klippel.de](http://www.klippel.de)
- [28] N. E. Iversen, H. Schneider, A. Knott and M. A. E. Andersen, "Efficiency Investigation of Switch-Mode Power Audio Amplifiers Driving Low Impedance Transducers", in AES Convention 139th, New York October 29th-1st November, 2015.